INTERNATIONAL JOURNAL FOR NUMERICAL METHODS IN FLUIDS
Int. J. Numer. Meth. Fluids **28**: 703–718 (1998)

A NUMERICAL METHOD FOR THE COMPUTATION OF THE EFFECTS OF AN AIR VESSEL ON THE PRESSURE SURGES IN PUMPING SYSTEMS WITH AIR ENTRAINMENT

T.S. LEE*

Mechanical and Production Engineering Department, National University of Singapore, 10 Kent Ridge Crescent, Singapore 119260, Singapore

SUMMARY

This paper describes an improved numerical method and computational procedure for the implementation of typical air vessel responses and their influence on the pressure transient for unsteady flow in a pipeline system with air entrainment. The proposed numerical method and computational procedure is without the necessity of an excessive iterative procedure as required previously by the conventional approach. The effects of air in the transient fluid system with the air vessel were then studied through the improved numerical computational method. Free and dissolved gases in the transported fluid, and cavitation at vapour pressure, are included. © 1998 John Wiley & Sons, Ltd.

KEY WORDS: pressure transient; air vessel; air entrainment; fluid system

1. INTRODUCTION

A common flow arrangement in water and sewage engineering consists of a lower reservoir, a group of pumps with a check valve in each branch, a pipeline discharging into an upper reservoir (water tower, gravity conduit, aeration well, etc.). In order to safeguard the pipeline and its hydraulic components from over and/or under pressurisation, it is important to determine extreme pressure loads under transient conditions. Pump stoppage is an operational case that has to be investigated and which often gives rise to maximum and minimum pressures. The most severe case occurs when all the pumps in a station fail simultaneously due to power failure. In this case, the flow in the pipeline rapidly diminishes to zero and then reverses. The pump also rapidly losses its forward rotation and reverses shortly after the reversal of the flow. As the pump speed increases in the reverse direction, it causes great resistance to the back flow, which produces high pressure in the discharge line near the pump. To prevent reverse flow through the pump, a check valve is usually fitted immediately after each pump. When flow reverses, the check valve is activated and closed. A large pressure transient occurs in the pipeline when the flow reverses and the check valve is rapidly closed.

When an air vessel is installed, it is usually used as a surge protection device for the unsteady flow conditions in the pumping system [1]. An air vessel is also known as air chamber or

* Correspondence to: Mechanical and Production Engineering Department, National University of Singapore, 10 Kent Ridge Crescent, Singapore 119260. Singapore.

CCC 0271–2091/98/140703–16$17.50

Received August 1996
Revised October 1997

volumetric tank. It is a vessel having compressed air at the top and liquid in its lower portion. The most common use of an air vessel is as a pressure surge control device, to limit the minimum transient pressure head in a pipeline system downstream of a group of pumps during the transient flow period following the pump(s) failure or shut down. In this case, the air vessel is placed immediately downstream of the pumps and of any check valves. In many applications, the air vessel is also designed to turn high frequency, high pressure transients into low frequency, low pressure oscillations in the fluid system. An air vessel has a number of advantages over both the open top surge tank and the valve-type surge suppresser. The air vessel can be built smaller than the open surge tank. Environmental problems associated with ambient pollution and debris in the open surge tank are avoided, and less space is generally required.

The air vessel installed on the pumping main, downstream of the group of pumps, is to prevent negative pressure and column separation in the pipeline systems downstream of the vessel. It consists of a scaled vessel, partially filled with fluid with the rest occupied by pressurised air. When pumps trip, fluid is drawn from the vessel into the pipeline and the volume of air within the vessel expands, causing the air pressure in the air vessel to drop. The rate at which the pressure in the air vessel drops is dependent on the initial air volume, the thermodynamic process that the air goes through, and the rate at which the liquid is being drawn out of the vessel. The air vessel must be large enough to supply the necessary volume of water to the pipeline during downsurge without reaching the point where air enters the line. The initial air volume inside the vessel must be sufficiently large for the air vessel to become an effective surge suppression device [2].

Based upon a knowledge of the physical characteristics of the pipeline to be protected, and the Joukowsky instantaneous flow stoppage pressure surge value, the frictional losses to be expected along the pipeline and the designer-specific allowable maximum and minimum pressure heads in the pipeline, the ESDU data and Graze and Horlacher charts [3] provide an estimate of the initial air volume ($\mathrm{Vol}_{\mathrm{ref}}$) required in the air vessel.

Charts [4] can also be used for the preliminary sizing of an air vessel needed for a pipeline system. These charts can be used to determine the size of an air vessel for a pipeline to keep the maximum and minimum pressures within design limits [5]. Usually, these charts make use of dimensionless system parameters, together with the maximum upsurge and minimum downsurge, to arrive at an initial air volume. The air vessel volume is obtained by giving an allowance factor to the initial air volume. This allowance is typically in the range of up to 25%. Throttling is usually not included in the above selection of the air vessel size. Graze and Horlacher [3] showed that air chambers are underutilised if optimum by-pass throttling is not included with the air chamber installation. However, throttling is usually done on inflow as throttling on outflow might cause column separation.

Detailed analysis of a pipeline system (Figure 1) with no air vessel was earlier studied by Lee [6,7]. The most severe case (all the pumps in the station failing simultaneously due to power failure) was analysed for the maximum and minimum pressure variations along the pipeline. In the present analysis, an air vessel is installed at B on the pumping main, located immediately outside of the pump house. Inside the pump house, the delivery main of each pump is attached to a check valve assembly (point A in Figure 1). When the pumps trip, forward flow diminishes to zero and the check valves are assumed closed at zero reverse flow.

The present work proposed an improved numerical method and computational procedure for the implementation of the responses of a typical air vessel (as shown in Figure 2) and its influence on the pressure transient for unsteady flow in a pipeline system with air entrainment. The proposed numerical method and computational procedure is without the necessity of an

excessive iterative procedure as required previously by the conventional approach. The effects of air in the transient fluid system with the air vessel are then studied through the improved numerical computational method. Free and dissolved gases in the transported fluid, and cavitation at vapour pressure are included.

2. NUMERICAL METHOD FOR THE COMPUTATION OF AIR VESSEL TRANSIENT RESPONSES IN A FLUID SYSTEM WITH AIR ENTRAINMENT

The method of characteristics applied to the above pressure transient problem, with variable wave speed (a_i) and any grid point (i, j) (Figure 3), can be described by the following finite difference expressions [8,9]

C^+ characteristics

$$\frac{g}{a_R}\frac{(H_i^{k+1}-H_R)}{\Delta t^k}+\frac{(V_i^{k+1}-V_R)}{\Delta t^k}+\frac{g}{a_R}V_R\sin\alpha_i+\frac{K_1}{2D}V_R|V_R|=0, \tag{1a}$$

$$\frac{x_i-x_R}{\Delta t^k}=V_R+a_R, \tag{1b}$$

and C^- characteristics

$$-\frac{g}{a_S}\frac{(H_i^{k+1}-H_S)}{\Delta t^k}+\frac{(V_i^{k+1}-V_S)}{\Delta t^k}-\frac{g}{a_S}V_S\sin\alpha_i+\frac{K_1}{2D}V_S|V_S|=0, \tag{2a}$$

$$\frac{x_i-x_S}{\Delta t^k}=V_S-a_S. \tag{2b}$$

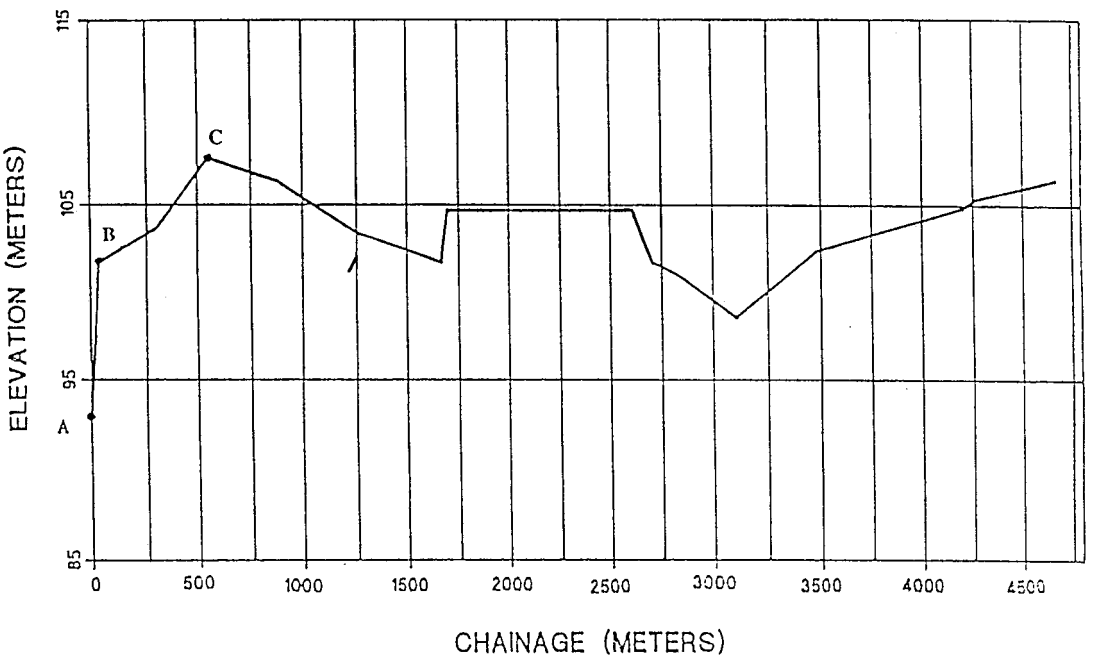

Figure 1. Pipeline profile.

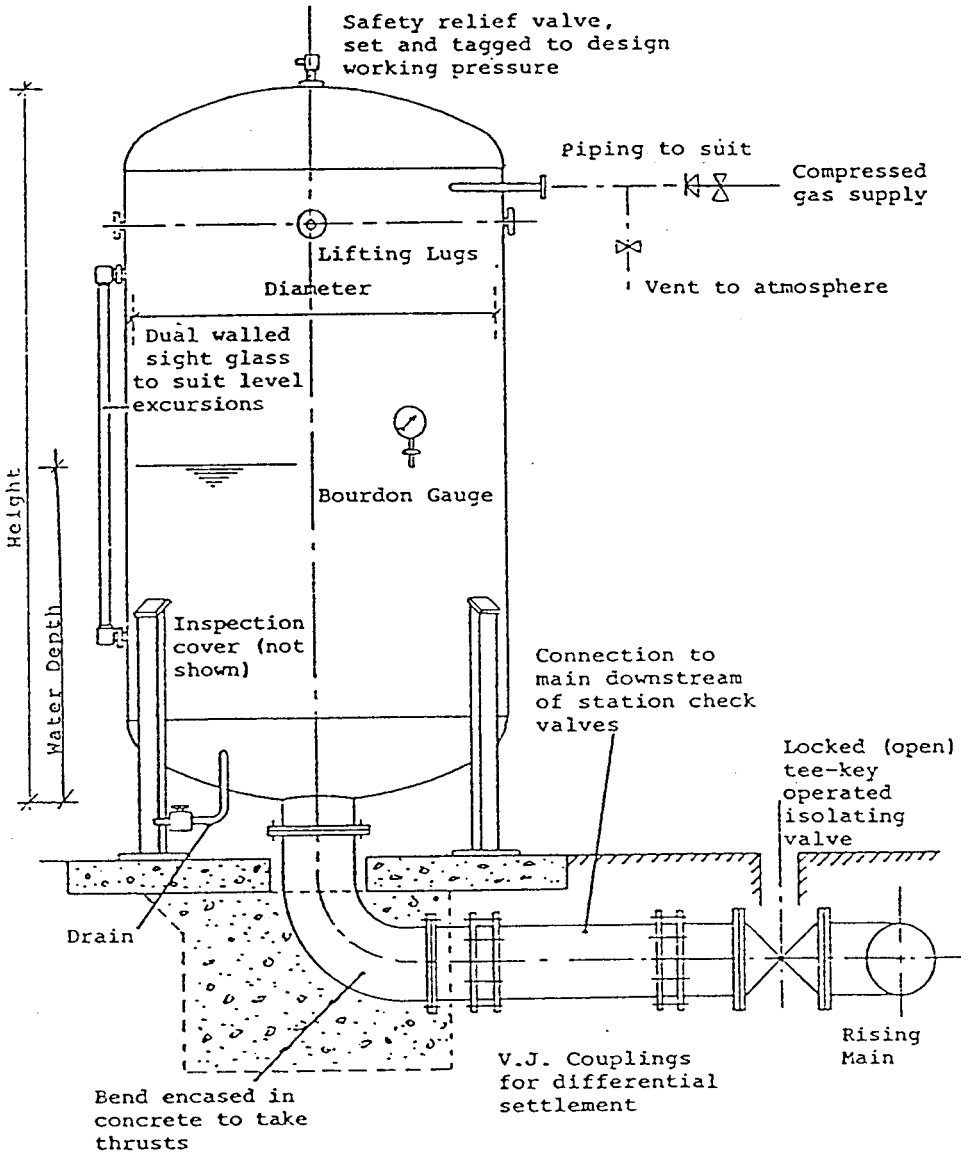

Figure 2. Air vessel installation at location B.

With conditions known at points $(i-1)$, i, $(i+1)$ at the kth time level, the conditions at R and S can be evaluated by a linear interpolation procedure. The conditions at R and S are then substituted into the Equations (1) and (2) and the solutions at the next $(k+1)$th time level at point i are obtained for $i = 0, \ldots, N_t$.

For an air vessel installed on the pipeline at a point B(i, j) (Figure 1) and at any instant of time, the initial pressure of the air in the air vessel as shown in Figures 2 and 3 expressed as equivalent height of water column $(H_w)^k$ is given by

$$(H_w)^k = H_i^k - Z_t - h_b - (h_t)^k + H_{atm}, \tag{3a}$$

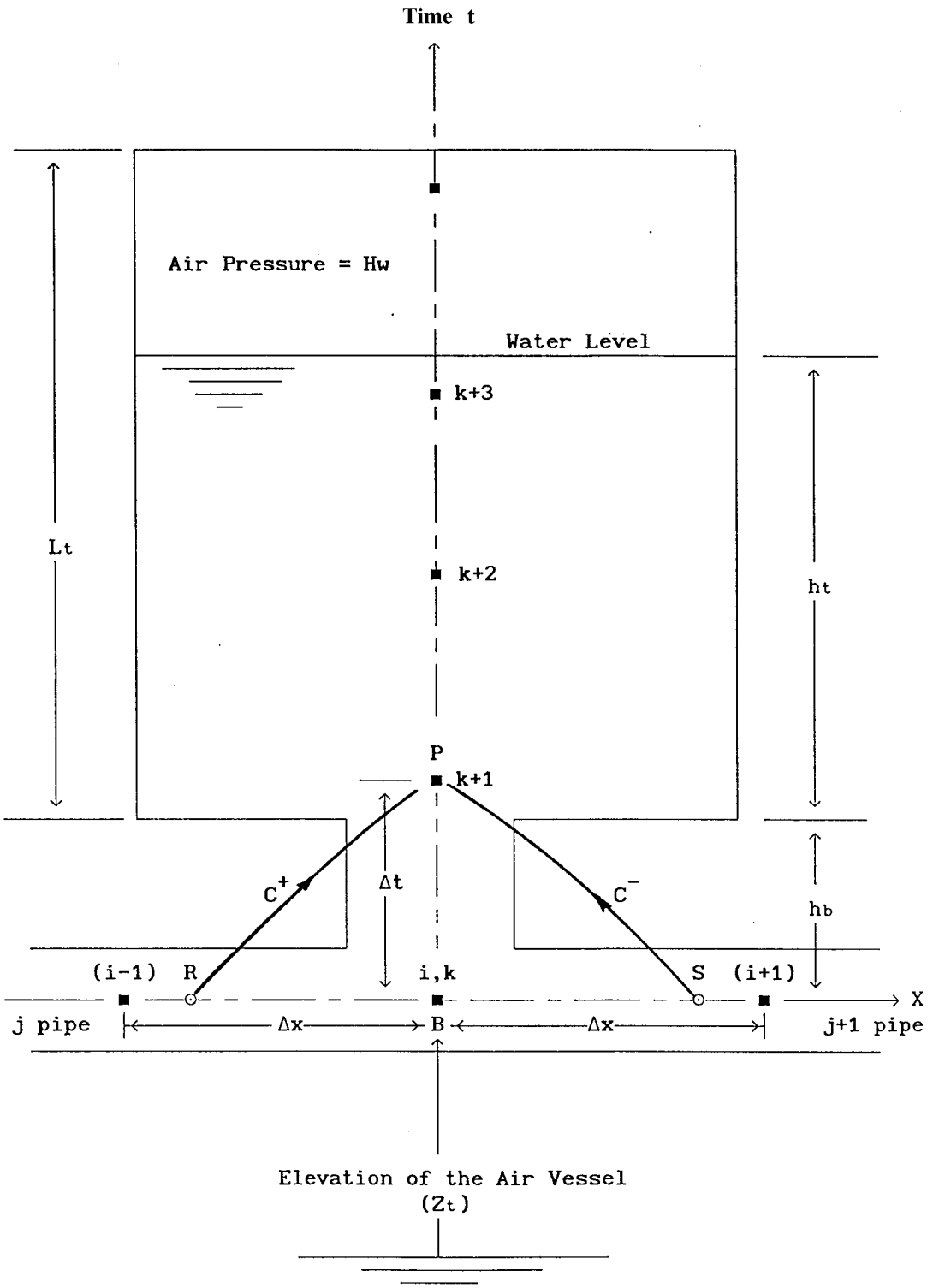

Figure 3. Schematic model and computational characteristics grid of air vessel at location B.

or

$$H_i^k = (H_w)^k + (h_t)^k + h_b + Z_t - H_{atm}. \tag{3b}$$

Applying a forward C^+ characteristic equation to the Δx segment upstream of the air vessel, the following equation is obtained

$$V_{i,j}^{k+1} = V_R - \frac{g}{a_R}(H_i^{k+1} - H_R) - \frac{g}{a_R} V_R \sin \alpha_R \, \Delta t - \frac{K_l \Delta t}{2D} V_R |V_R|. \tag{4}$$

By applying a backward C^- characteristic quotation to the Δx segment downstream of the air vessel, the following equation is obtained

$$V_{i,j+1}^{k+1} = V_S - \frac{g}{a_S}(H_i^{k+1} - H_S) - \frac{g}{a_S} V_S \sin \alpha_S \, \Delta t - \frac{K_l \Delta t}{2D} V_S |V_S|. \tag{5}$$

The transient wave speed a_i, with a fraction content of ε_i is given by

$$a_i^k = \left\{ \rho_w (1 - \varepsilon_i^k) \left[\frac{1}{K} + \frac{\varepsilon_i^k}{n P_i^k} + \frac{cD}{eE} \right] \right\}^{1/2}. \tag{6}$$

The transient computation of the fraction of air content along the pipeline depends on the local pressure and air volume and is given by

$$\varepsilon_T^{k+1} = \left\{ \frac{P_i^k}{P_i^{k+1}} \right\}^{1/n} \varepsilon_i^k \quad \text{and} \quad \varepsilon_0^{k+1} = \left\{ \frac{P_0}{P_i^{k+1}} \right\}^{1/n} \varepsilon_0, \tag{7}$$

for $P_i^{k+1} \geq P_g$ and $\varepsilon_T^{k+1} \leq (\varepsilon_0^{k+1} + \alpha_{gr} \varepsilon_g)$

$$\varepsilon_i^{k+1} = \varepsilon_T^{k+1}, \tag{8a}$$

for $P_i^{k+1} \geq P_g$ and $\varepsilon_T^{k+1} > (\varepsilon_0^{k+1} + \alpha_{gr} \varepsilon_g)$

$$\varepsilon_i^{k+1} = \left\{ \frac{P_i^k}{P_i^{k+1}} \right\}^{1/n} (\varepsilon_i^k + \alpha_{ga} \varepsilon_g), \tag{8b}$$

for $P_i^{k+1} < P_g$

$$\varepsilon_i^{k+1} = \left\{ \frac{P_i^k}{P_g} \right\}^{1/n} (\varepsilon_i^k + \alpha_{gr} \varepsilon_g). \tag{8c}$$

The theoretical derivation and assumptions made for Equations (7) and (8) are given in [6]. For water saturated at atmospheric pressure, the gas release pressure head approaches that of the vapour pressure (i.e. 2.4 m water absolute). Typical free air content in sewage at atmospheric pressure is about 0.1%, the free gas content evolved at the gas release head is about 2.0% at atmospheric head. The fraction of gas absorption is $\alpha_{ga} = 0.3$ and the fraction of gas release is $\alpha_{gr} = 0.6$ [10]. Most of the existing computations of the fluid system with air vessel installations do not include the air entrainment computation, which can produce incorrect predictions of the transient behaviours as will be shown by the present computations.

For the continuity requirement

$$A_{p_j} V_{i,j}^{k+1} = A_t \frac{dh_t}{dt} + A_{p_{j+1}} V_{i,j+1}^{k+1}. \tag{9}$$

Thus,

$$(\Delta h_t)^{k+1} = [A_{p_j} V_{i,j}^{k+1} - A_{p_{j+1}} V_{i,j+1}^{k+1}] \frac{\Delta t}{A_t}. \tag{10}$$

Through finite difference approximation, the depth of liquid at the end of the time interval Δt is given by

$$(h_t)^{k+1} = (h_t)^k + (\Delta h_t)^{k+1}, \tag{11}$$

where $(h_t)^k$ is the depth of liquid in the air vessel at the beginning of the Δt interval. Hence,

$$V_a^{k+1} = V_a^k + A_t (h_t)^{k+1}. \tag{12}$$

The new pressure head in the air vessel is obtained from

$$\begin{aligned} &P_a^k \{V_a + \tau(t)[E_1 + E_2(P_a/P_0) + E_3(P_a/P_0)^2]\Delta t\}_k^n \\ &= P_a^{k+1} \{V_a + \tau(t)[E_1 + E_2(P_a/P_0) + E_3(P_a/P_0)^2]\Delta t\}_{k+1}^n, \end{aligned} \tag{13}$$

where τ, E_1, E_2 and E_3 are the characteristics of air inflow/outflow device if the air vessel is fitted with air valves or other air supply lines responding to the transient flow in the fluid system.

In estimating the gas expansion characteristics within the air vessel, an appropriate value of the polytropic coefficient of expansion must be selected. Values in the range 1.0–1.4 are normally utilised. Thorley [11] recommended a value of 1.3–1.4 if little or no heat transfer is expected and values closer to 1.0 if significant heat transfer occurs, effectively rendering the process isothermal.

To restrict the inflow into or outflow from the chamber, an orifice is usually provided between the chamber and pipeline. A ratio of 2.5:1 between the orifice losses for the small inflow and outflow is commonly used. Allievi [12], Angus [13] and Evans and Crawford [5] are some of the historical works on the use of air chambers in pumping stations to control transients generated by power failure to the pumps.

Equation (13) is valid only over a very short interval of time specified by a Δt value. The value of $n = 1.0$ (isothermal) is used for 'slow' processes, while $n = 1.4$ (adiabatic) is assumed for 'fast' transient systems. The difference in the extreme transient pressure response of a fluid system can be of the order of 20% [3] for different value of n used.

Finally,

$$(H_w)^{k+1} = P_a{}^{k+1}/\rho_w g, \tag{14a}$$

$$H_i^{k+1} = (H_w)^{k+1} + (h_t)^{k+1} + h_b + Z_t - H_{atm}. \tag{14b}$$

The above method of computation from Equations (3)–(14b) do not require an iterative procedure as would normally be required if a different formulation for the model of the air vessel was used [9].

The value of the time step Δt_k at each time level is determined by the CFL criterion

$$\Delta t^k = \min\left\{k_i \frac{\Delta x}{(|V_i| + a_i)}\right\} \quad \text{for} \quad i = 0, 1, \ldots, N. \tag{15}$$

where k_i is a constant less than 1.0.

With reference to the time- and x-grid notation used in Figure 3, i denotes the x-mesh point at location $x = (i, \Delta x)$ and k denotes the time level corresponding to time at $t^k = \Sigma(\Delta t^k)$.

3. INITIAL AND TRANSIENT BOUNDARY CONDITIONS

The initial steady state pressure head (H) along the pipeline and flow rate (Q_0) in the system are determined from the system characteristics and the characteristics of the pumps for the pumping station. The equivalent pump characteristics in the pumping station during pump stoppage and pump rundown can be described by the homologous relationship for n_p pumps as follows [7]

$$H_e^{k+1} = A_1(N^{k+1})^2 + (A_2/n_p)(N^{k+1})Q_0^{k+1} + (A_3/n_p^2)(Q_0^{k+1})^2, \tag{16}$$

$$T_e^{k+1} = (B_1 n_p)(N^{k+1})^2 + B_2(N^{k+1})Q_0^{k+1} + (B_3/n_p)(Q_0^{k+1})^2, \tag{17}$$

$$\eta_e^{k+1} = C_1 + (C_2/n_p)(Q_0^{k+1}/N^{k+1}) + (C_3/n_p^2)(Q_0^{k+1}/N^{k+1})^2, \tag{18}$$

$$T_e = -I_e \frac{d\omega}{dt}, \tag{19}$$

with $H_0^{k+1} = H_e^{k+1}$; $I_e = n_p I$; $\omega = 2\pi N$; $Q =$ flow rate; $n_p =$ number of pumps; A_1, A_2, A_3; B_1, B_2, B_3 and C_1, C_2, C_3 are single pump constants; H_e, T_e, η_e are the equivalent pump head, torque, and efficiency, respectively. The efficiency of the equivalent pump during pump rundown is assumed equal to the efficiency of the corresponding single pump rundown. Equation (15) is to be solved together with the C^- characteristics line described by Equations (13) and (14) for a pump speed N^{k+1}, which was determined from Equations (16)–(18) following the procedures Fox [9] by using the concept of an equivalent pump when there is more than one pump operating in a pumping station. The change in pump speed during pump rundown for both normal and turbine modes are modelled. When reversed flow is encountered in the pump, the check valve is assumed closed. At this instant, V_0^{k+1} is assumed zero for the C^- characteristic line at $i = 0$ for all subsequent time levels. In the case where the check valve closing time is known, the flywheel or pumpset inertia can be sized, so that the pump continues delivery for a period longer than the check valve closure time. This will ensure non-reversal of flow before the check valve is able to close. Downstream of each of the above profiles is assumed a constant head reservoir, i.e. H_N^{k+1} is a constant for all time levels and this is solved with the C^+ characteristic line for V_N^{k+1} for each time level.

The computational procedure for all of the above starts with an analysis of the pressure head (H) and flow rate (Q_0) of the steady state fluid system with the air vessel attached at point B. The operating pumps of the pumping station are then tripped at time $t = 0$ (time level $k = 0$). The rundown characteristics (H, Q, N, T and η) of the equivalent pump are then obtained. The transient characteristics of the fluid system are computed from $i = 0$ to $i = N$. When the computation arrives at the point where the air vessel is installed, the governing equations related to the air vessel characteristics are then implemented. At point $i = N$, the boundary condition of a fixed reservoir is imposed. At another time level $(k + 1)$, the process is repeated with a new set of the equivalent pump characteristics imposed at $i = 0$. The process is then repeated for a predetermined transient time. During the transient calculation for the fluid system, the computation of the air vessel characteristics is determined by the model proposed by Equations (3)–(13). The results obtained in this work are for a computation with mesh points $N = 1001$.

4. RESULTS AND DISCUSSION

Initially, the effects of air entrainment on pressure transients generated by the simultaneous trip of all pumps operating in a pumping station, with the undulating pipeline contour as shown in Figure 1, were investigated for a vertical air vessel installed at point B along the pipeline profile. The pumping station uses three parallel centrifugal pumps to supply 1.08 $m^3 s^{-1}$ of water to a tank 19.7 m above the sump level, through a 0.985 m diameter main of 4720 m length. The pumpset moment of inertia (including the flywheel) was studied for an equivalent pumpset moment of inertia of $I_e = 0.1$, 0.5, 1.0, 2.0, 5.0 and 10 of a reference pumpset inertia (I) of 99.9 kg m^2. The air void fraction (ε) studied was in the range 0.00–0.03.

Figures 4–6 show the effects of air entrainment on the pressure transients at a point C (at the peak) of the pipeline contour for different equivalent pumpset moments of inertia. Five distinct pressure transient characteristics were observed from the above numerical experiments: (i) The pressure peak varies with the ε and is greater than that predicted by the constant wave speed model ($\varepsilon = 0.000$) with the transient times that occur differing. (ii) The damping of surge pressure is noticeably larger with $\varepsilon > 0.000$ when compared with the constant wave speed model ($\varepsilon = 0.000$). (iii) With $\varepsilon > 0.000$, the pressure surges are asymmetric with respect to the static head, while the pressure transients for the constant wave speed model are symmetric with respect to the static head. (iv) When air was entrained into the system, the pressure transient showed long periods of downsurge and short periods of upsurge when compared with the gas-free constant wave speed case. From past experiences, surge measurements [7,14] indicate that the damping is faster in reality, indicating that more energy dissipating mechanisms than the ordinary friction are at hand. (v) The degree of amplification of the first pressure peak is dependent upon the rate of deceleration of the flow after the pump trip. An increased pump inertia (by attaching a flywheel to the driveshaft) generally produces a smaller amplification of the first pressure peak as compared with the constant wave speed model.

Figures 4–6 also show that increasing the air vessel volume results in significant damping of the peak or maximum pressures in the pipeline. There is a peak in the maximum pressure that will eventually damp down to the static head of the fluid system. However, it should be pointed out that, if the pumpset inertia is low, the air vessel may behave as a poor pressure surge suppresser. Thus, an air vessel is an effective surge suppresser if and only if the pumpset inertia is sufficiently large to prevent pressure from the discharge side of the pump from falling below the suction. This implies that the air vessel requires a certain amount of pressure difference between its local pressure and the pressure at the pump before it responds to suppress the pressure transient. For low inertia, the rate of decrease of the pump head was so rapid that it prevented the air vessel from producing any significant effects.

With increasing air vessel volume, the frequency of the pressure surges decreases as the air vessel volume increases. This is because the air in a larger air vessel is compressed or expanded less severely as compared with a smaller one. In designing an air vessel, it is important to determine the minimum and maximum air volume in the air vessel. There must always be adequate air in the air vessel to control the surges to the desired limits, and there must also be enough water in the air vessel to prevent air from entering the pipeline.

Figures 4–6 further show that, for a given pumpset inertia, the maximum pressure peaks need not necessarily occur at the minimum or maximum air entrainment levels. It can occur at an intermediate critical range of air entrainment value. This range of critical air entrainment value can only be obtained through numerical experimentation for a given pumping system.

Figure 7 shows that the pumping system with an air vessel and entrained, entrapped or released gases significantly alter the flow reversal time. From the available flow reversal time,

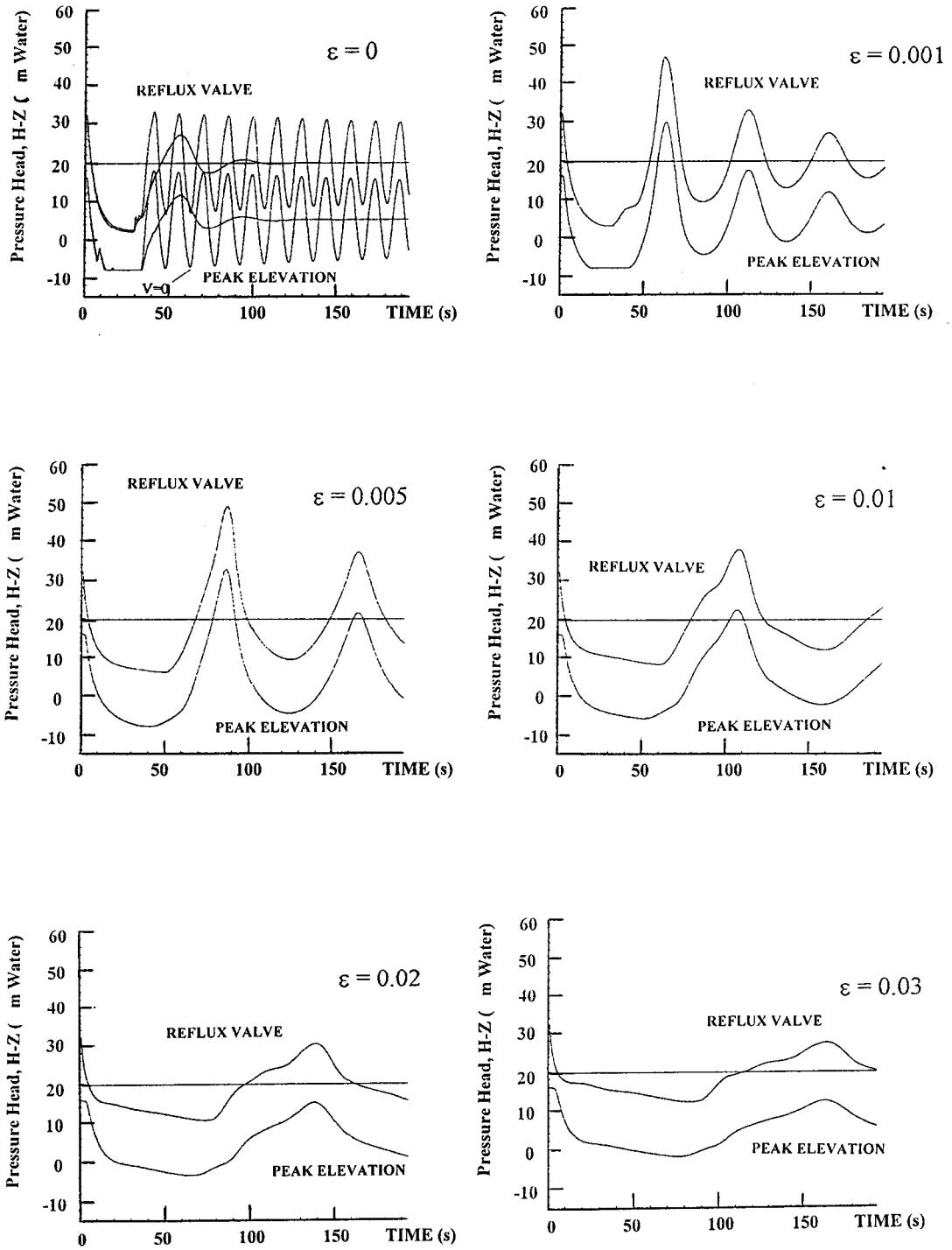

Figure 4. Pressure transients immediately downstream of check valve (A) and at the peak location of the pipeline (C) (air vessel volume = 0.5 Vol_{ref}).

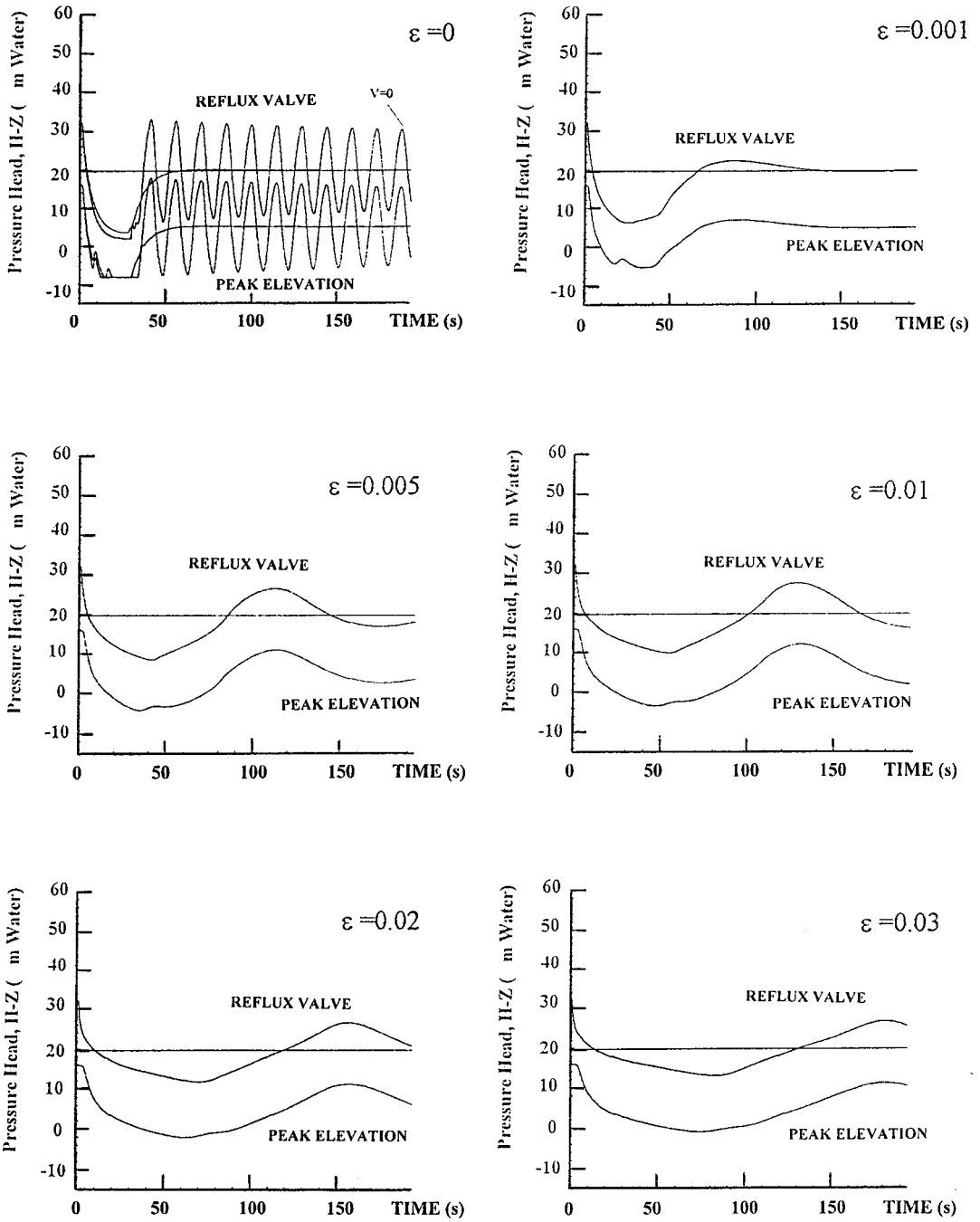

Figure 5. Pressure transients immediately downstream of check valve (A) and at the peak location of the pipeline (C) (air vessel volume = 1.0 Vol_{ref}).

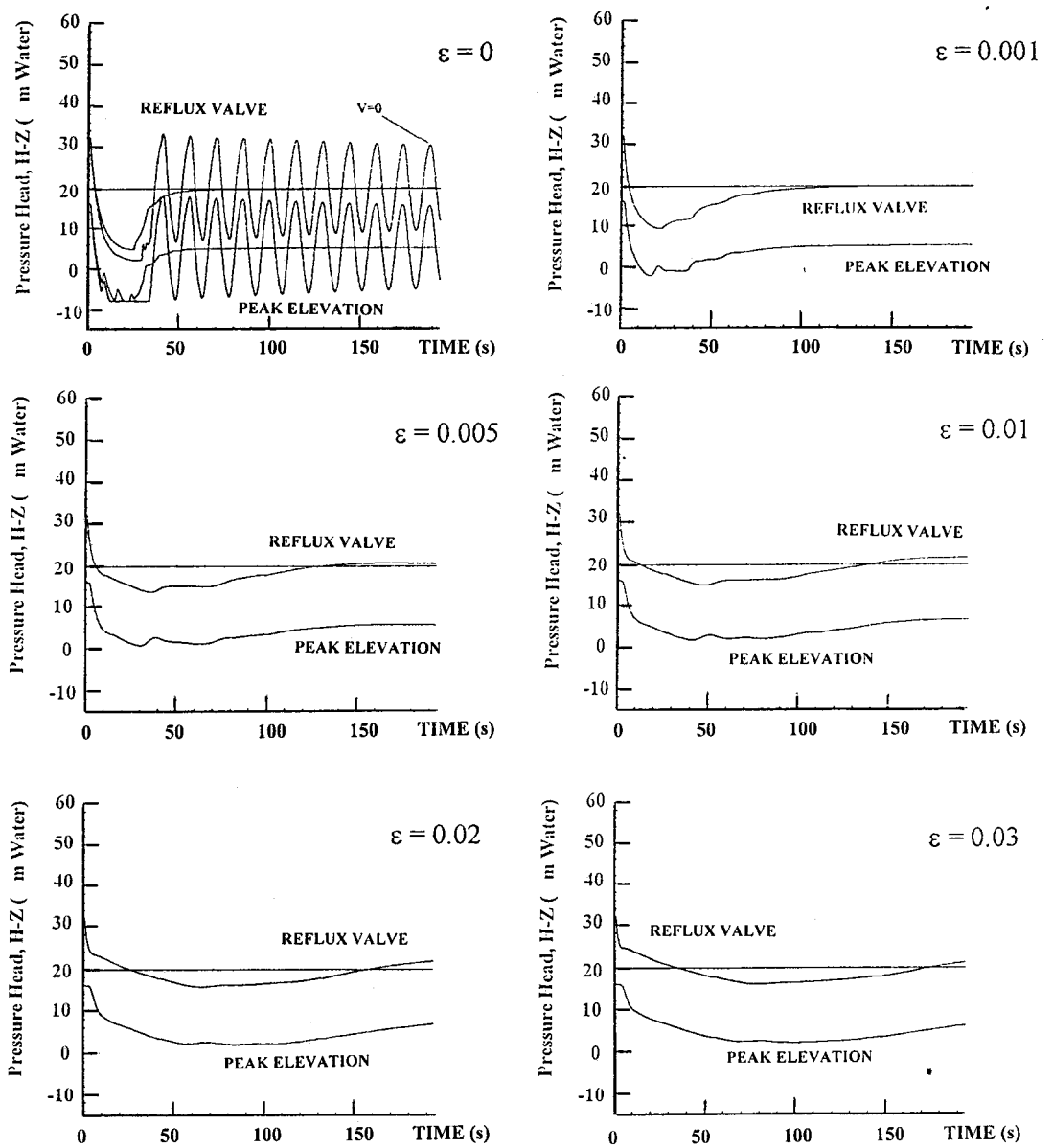

Figure 6. Pressure transients immediately downstream of check valve (A) and at the peak location of the pipeline (C) (air vessel volume = 5.0 Vol_{ref}).

the reverse flow velocity gradient with respect to time is obtained. The results presented in Figure 7 show that the effects of the check valves in transient flow can be predicted by means of numerical computation of the equivalent flow reversal time. When analysing these effects, both steady flow rate and fluid velocity gradient with time have to be considered. For systems with large flow rates, the fluid velocity gradient is important. The time interval necessary for flow reversal and mode of the flow rates versus time variation during the flow reversal period gives an indication of the necessary characteristics for a satisfactory flow and pressure

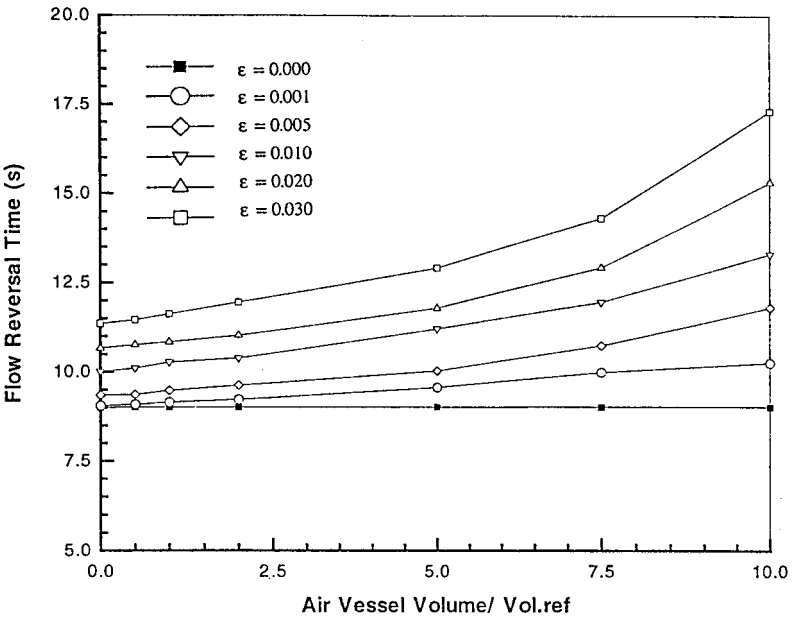

Figure 7. Effects on flow reversal time.

predictions for the check valve closure. The above observations through numerical experiments are consistent with field measurements and observations [7,14] of pressure surges in prototype pumping stations at various modes of pumps operating under normal conditions and pumps operating near low water cut-out levels with air entrainment due to attached surface vortices. Observations showed that the commonly used swing check valve close when flow reversed. At the instant of valve closure, a large pressure variation was initiated.

Figure 8 shows that, with no air vessel in the fluid system, as the air entrainment value, ε, increases, the pressure peak decreases. Chaudhry *et al.* [8], through extensive experimental work, obtained very similar conclusions. Detailed mechanisms of the effects of air entrainment on a fluid transient system are given in Reference [6]. Briefly, they are caused by the increased bulk viscosity of the fluid due to air bubbles, losses due to slip between bubbles and water, the thermodynamic effects, the expansion and contraction processes of the air bubbles, the processes of absorption of free air and release of dissolved air within the fluid system due to the variation of the transient pressure, etc.

In general, the peak pressures throughout the pipeline profile decreased with the introduction of an air vessel as compared with one without. The air vessel lowers the high transient pressure at reverse flow by allowing water beyond the air vessel to flow into the air vessel instead of accelerating towards the closed check valve. The air vessel also reduces the pressure during pump rundown by feeding water into the pipeline. The air vessel also regulates the upsurge and downsurge by allowing the air mass within the air vessel to dissipate the energy of the pressure surges through compression and expansion of the air volume. As the air vessel volume increases, the magnitude of the peak pressures and the magnitude of the downsurge throughout the pipeline decreases. The acceleration and deceleration of the flow into and out of the air vessel are very slow if the air vessel volume is large. A bigger air vessel would also be a better surge suppresser because it has a larger initial air mass, so that there could be greater compression or expansion of the air resulting in greater dissipation of the energy of the pressure surges and thus lower peak pressures.

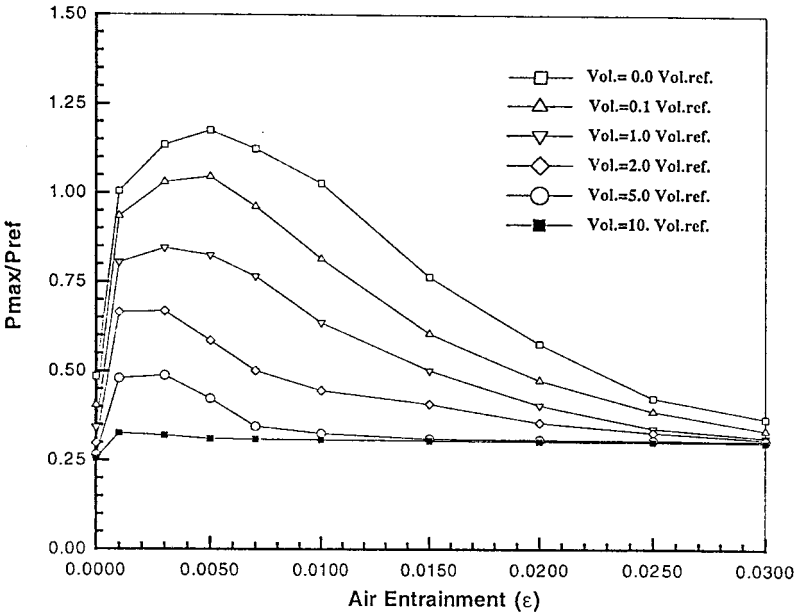

Figure 8. Effects on maximum transient pressure.

5. CONCLUSIONS

The proposed numerical method for the computation of transient flow in a fluid system with air vessel shows that the characteristics of the pressure surges with various modes of pump operation can be predicted by means of a computational procedure for the flow characteristics of the air vessel. The proposed numerical method is without the necessity of an excessive iterative procedure as required previously by the conventional approach. The effects of air in the transient fluid system with the air vessel were studied through the improved numerical computational method. Free and dissovled gases in the transported fluid, and cavitation at vapour pressure are included. Numerical experiments showed that entrained, entrapped or released gases in the transient fluid system without an air vessel tend to amplify the first pressure peak, increase surge damping and produce asymmetric pressure surges with respect to the static head. The pressure transient also showed long periods of downsurge and short periods of upsurge. The upsurge was considerably amplified and down-surge was marginally reduced when compared with the gas-free case. Numerical experiments show that the maximum transient pressure can be considerably reduced if an appropriately sized air vessel is chosen. The results obtained are in qualitative agreement with observations from former field measurements.

ACKNOWLEDGMENTS

The kind assistance of the personnel from the Sewerage Department, Ministry of the Environment, Singapore is gratefully acknowledged for providing valuable information on pumping stations for this investigation. The support of a National University of Singapore research Grant (No. RP890633) is also gratefully acknowledged.

APPENDIX A. NOMENCLATURE

a	wave speed
A_p	cross-sectional area of the pipe
A_t	cross-sectional area of the tank
A_1, A_2, A_3	constants for pump H–Q curve
B_1, B_2, B_3	constants for pump T–Q curve
C_1, C_2, C_3	constants for pump η–Q curve
c	parameter describing pipe constraint condition
d_i	internal diameter of the pumping main
d_t	internal diameter of the air vessel
D	mean diameter of the pipe
E	modulus of elasticity
e	local pipe-wall thickness
f	friction factor
g	gravitational acceleration
h_b	height of the base of the tank above the centre line of the pipe line where the air vessel is located
h_t	height of water in the tank
H	gauge piezometric pressure head
H_{atm}	atmospheric pressure
H_g	gas release pressure head (= 2.4 m water absolute)
H_w	absolute pressure of the air in the air vessel expressed as an equivalent height of water column
i	node point at $x_i = (i-1)\Delta x$
I	pumpset moment of inertia including flywheel
k	time level at $t^k = \Sigma\, \Delta t^k$
K	bulk modulus of elasticity
K_l	pipe loss coefficient (including friction and minor losses)
L_t	longitudinal length (height) of the air vessel
L	length of pipe
n	a polytropic coefficient of expansion and contraction
n_p	number of pumps in a pumping station
N	pump speed in rpm at node point i and time level
N_t	total number of node points along the pipeline
p	gauge pressure inside the pipe
P	absolute pressure
P_a	absolute pressure of the air in the air vessel
P_0	a reference pressure in the air vessel
P_g	gas release pressure
Q	fluid flow rate
Re	Reynolds number
R	C^+-line interception on x-axis at kth time level
S	C^--line interception on x-axis at kth time level
T	pump torque
t	instantaneous time in transient flow
V	flow velocity

V_a	volume of air in the air vessel at pressure P_a
V_t	flow velocity in the pipe leading to the air vessel
V_p	flow velocity at the junction leading to the air vessel at the next time level
x	distance along pipeline
z	pipeline elevation with respect to pump intake level
Z_t	elevation above datum of the centre line of the pumping main at the point of its junction with the tank

Greek letters

α	pipeline inclination (positive downward)
α_{ga}	fraction of gas absorption
α_{gr}	fraction of gas absorption
η	pump efficiency
τ	valve closure function
Δt^k	time step at k-time level
Δx	node point distance along pipeline
v_s	sewage kinematic viscosity
v_g	gas kinematic viscosity
ε	fraction of air in liquid
ε_0	fraction of free gas in liquid at atmospheric pressure
ε_g	fraction of dissolved gas in liquid
ρ_w	density of fluid

REFERENCES

1. D.S. Clarke, 'Surge suppression—a warning', *Proc. Int. Conf. on the Hydraulics of Pumping Stations*, Manchester, UK, 1985, pp. 39–54.
2. C.S. Martin, 'Method of characteristics applied to calculation of surge tank oscillations', *Proc. Int. Conf. on Pressure Surges*, University of Kent, Canterbury, UK, 1972, pp. E1-1–E1-12.
3. H.R. Graze and H.B. Horlacher, 'Design charts for throttle (by-pass) air chambers', *5th Int. Conf. on Pressure Surges*, Hannover, Germany, 1986, pp. 309–322.
4. A.T.K. Fok, 'Design charts for air chamber on pump pipe lines', *ASCE J. Hydraul. Div.*, **HY9**, 1289–1302 (1978).
5. W.E. Evans and C.C. Crawford, 'Design charts for air chambers and pump lines', *Trans. Am. Soc. Civil Eng.*, **119**, 1025–1045 (1954).
6. T.S. Lee, 'Numerical modelling and computation of fluid pressure transients with air entrainment in pumping installations', *Int. j. numer. methoids fluids*, **19**, 89–103 (1994).
7. T.S. Lee, 'Numerical studies on effects of check valve performance on pressure surges during pump trip in pumping system with air entrainment', *Int. j. numer. methods fluids*, **21**, 337–348 (1995).
8. M.H. Chaudhry, S.M. Bhallamudi, C.S. Martin and M. Naghash, 'Analysis of transient pressures in bubbly, homogeneous, gas–liquid mixtures', *ASME J. Fluid Eng.*, **112**, 225–231 (1990).
9. J.A. Fox, *Hydraulic Analysis of Unsteady Flow in Pipe Network*, Macmillan, London, 1984.
10. I.S. Pearsall, 'The velocity of water hammer waves', *Symp. Surges in Pipelines*, *Proc. Inst. Mech. Eng.*, **180**, 12–20 (1965/66).
11. A.R.D. Thorley and P. Lastowiecki, 'Air vessel design for rising mains', *Proc. Int. Conf. on the Hydraulics of Pumping Stations*, Manchester, UK, 1985, pp. 89–98.
12. L. Allievi, 'Air chamber for discharge lines', *Trans. Am. Soc. Mech. Eng.*, **59**, 651–659 (1937).
13. R.W. Angus, 'Air chambers and air valves in relation to water hammer', *Trans. Am. Soc. Mech. Eng.*, **59**, 661–668 (1937).
14. L. Jonsson, 'Maximum transient pressures in a conduit with check valve and air entrainment', *Int. Conf. on the Hydraulics of Pumping Stations*, The University of Manchester, Institute of Science and Technology (UMIST) and HBRA—The Fluid Engineering Centre, Manchester, UK, 1985, pp. 55–76.

